4th Flow Control Conference
23 - 26 June 2008, Seattle, Washington

AIAA 2008-3761

An Experimental Investigation of a Jet and Vortex Actuator for Active Flow Control

Hasan Gunes[1] and Sertac Cadirci[2]
Istanbul Technical University, Istanbul, Turkey, 34437

Ulrich Rist[3]
Universität Stuttgart, Stuttgart, Baden-Württemberg, D-70550, Germany

An oscillatory, zero-net-mass flux Jet and Vortex actuator (JaVA) was built and tested in a still water tank. The striking feature of this JaVA model is that it can produce different flow types ranging from vertical through oblique to wall-parallel jets or vortices mainly depending on the chosen actuation frequency and amplitude. These flow types have been investigated using flow visualizations and by extracting quantitative velocity data using a gradient-based optical flow concept. The temporal behavior of basic JaVA-induced flow types have been further investigated using Fourier analysis. All quantitative features mentioned in Ref. 3 have been reproduced but our results are much more detailed and consist of instantaneous velocity fields for quantitative analysis. In addition, we have found that the actuator plate's mean position is another important parameter which significantly affects the JaVA-induced flow types.

Nomenclature

a	=	actuator plate amplitude	ν	=	kinematic viscosity
b	=	plate width of the actuator	Re	=	Reynolds number
f	=	frequency	S_a	=	scaled amplitude
g_n	=	ratio of narrow gap to plate width	t	=	time
g_w	=	ratio of wide gap to plate width	u	=	velocity component in x direction
I	=	image intensity	v	=	velocity component in y direction
K	=	actuator plate mean position	V_{max}	=	maximum velocity magnitude
N_1	=	number of pixels in x direction	w_n	=	narrow gap
N_2	=	number of pixels in y direction	w_w	=	wide gap

I. Introduction

THIS paper focuses on the JaVA-induced flow types and their numerical evaluation for a quantitative processing of the results. The JaVA could become a highly flexible active flow control device for boundary layer control. Conventional flow control devices, like vortex generators, are mostly passive which means that they do not need energy input, and that they do not react on the actual state of the flow[1]. Thus, vortex generators as conventional passive control devices/elements are simple in design and effective to prevent flow separation[2]. These devices are cheap to manufacture but they have two disadvantages: they are fixed and cannot be fully optimized for a single flight condition because of other flight conditions with different requirements, such that they cause extra drag in these other situations where they are no longer needed.

An active flow control device, like the present JaVA, on the other hand, are *active* flow control devices which are intended to overcome these disadvantages to enable longer aircraft range, manoeuvrability, stability and enhanced overall performance. Such a device adds only negligible drag when the system is not actuated and it does not need any external fluid if it is a zero-net-mass flux system. The present JaVA-device, originally proposed by

[1] Assoc. Prof. Dr., Department of Mechanical Engineering, Gumussuyu – Istanbul / guneshasa@itu.edu.tr.
[2] Research Assistant, Department of Mechanical Engineering, Gumussuyu – Istanbul / cadircis@itu.edu.tr.
[3] Prof. Dr.-Ing, Institut für Aerodynamik und Gasdynamik, Pfaffenwaldring 21 / rist@iag.uni-stuttgart.de

Lachowicz *et al.*[3] enables to achieve different flow regimes when it is operated at different amplitudes and frequencies. Thus, for different flight conditions, a desired flow regime that provides optimum flow control could perhaps be selected. With a better understanding of the interaction with boundary layers, a successful application of a JaVA system may lead to efficient flight control systems, such that manoeuvrability, stability and longer aircraft range might become possible at reduced costs[3].

The basic JaVA-induced flow types are reported in Ref. 3 as "free jets", "wall jets" and "vortex flows". In addition, we classify free jets as *"vertical", "oblique right"* and *"oblique left"*, and we also observe wall jets in either direction, as well as clockwise and anti-clockwise rotating vortex flows. It should be mentioned that the above flows originate from the wide slot of the actuator. However, depending on the mean position of the actuator plate, both wall and angled jets are also observable from the narrow slot. So, a lot of different regimes are possible depending on the parameter space. Wall jets are capable of direct flow-separation control[4]. Another achievement of active flow control is that additional/controlled vorticity generation enhances boundary-layer momentum transport and thus suppresses stall for compressible and incompressible flows[5].

II. Experimental Setup

The JaVA system in this study is based on the work stated in Ref. 3 in which a qualitative flow-field characterization of the JaVA system in still *air* is reported. In the present study, on the other hand, a similar but larger JaVA is designed and built to be tested in a *water* tank. Since we test the JaVA in water, we are able to use a much larger model. This leads to the use of larger actuator-plate amplitudes and a decrease of the actuator plate frequency to as low as *1 Hz* in turn, where we still can generate potentially useful flow regimes. Thus, real time visualizations of JaVA-induced flows are clearly observable and recorded with a camera. An image acquisition system consisting of a high-speed camera, a recording system, a class 3b visualization laser and red dye as tracer are the main tools for visualization of different flow regimes.

The current JaVA body is a Plexiglas cavity with an eccentrically mounted actuating plate which moves up and down like a piston as shown schematically in Fig. 1. Except for the driving system, the JaVA operates under water as shown in Fig. 2. Since the water is incompressible and the JaVA is a zero-net-mass flux system, the actuator plate acts like a piston pumping water in and out from the JaVA cavity. The vertical periodic motion of the actuator plate is realised by eccentric rotating discs (tappets) with various eccentricities a, driven by a low-frequency step motor. So, it is possible to precisely control the frequency of the plate motion. The actuator plate may have various widths (b = 21.8, 23.7, 25, 25.8 and 26.6 mm) which define one geometric parameter of the JaVA.

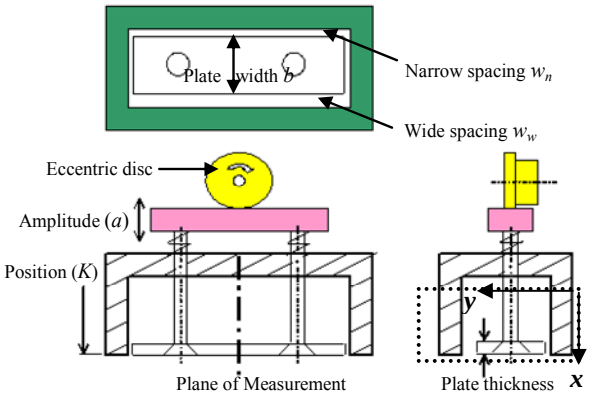

Figure 1. Scheme of JaVA device

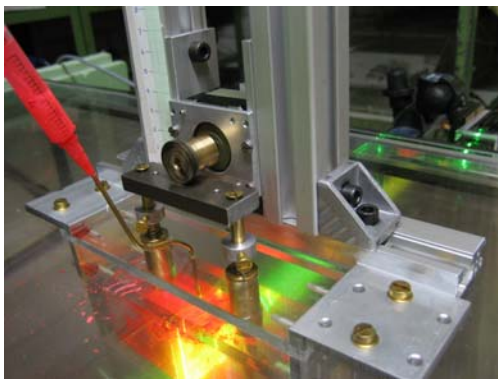

Figure 2. JaVA in water

The actuator plate is placed asymmetrically with respect to the JaVA body, thus there is a narrow and a wide slot between the plate and the body. Depending on the wide/narrow slot spacing w_w/w_n, actuator plate width b, the tappet's amplitude a, the frequency f and the mean actuator-plate position K, one can obtain different flow types such as oblique, vertical and wall jets as well as vortex flows. Following Ref. 3, we characterize the JaVA-induced flows based on the following dimensionless parameters; the ratios of narrow and wide slots to the actuator's plate width ($g_n = w_n/b$ and $g_w = w_w/b$), the scaled amplitude ($S_a = 2\pi a/b$), and the Reynolds number ($Re = 2\pi afb/\nu$). In

addition to these parameters, we have found that two other geometric parameters (namely the mean actuator-plate position and the plate thickness) are also important in the characterization and understanding of the flow types. In this paper, therefore, we report on the effect of the mean actuator-plate position as well as the Reynolds number on the JaVA-induced flows. In this study, all other parameters are kept constant. That is, the ratios of narrow and wide gaps to the plate width are $g_n = 0.012$ and $g_w = 0.1$, respectively and the scaled amplitude of the actuator plate is kept fixed at $S_a = 0.32$ ($a = 1.28$ mm, $b = 25$ mm).

III. Velocity Estimation Using Optical Flow

The visualisation images recorded by a camera can be used for quantitative image processing based on the concept of optical flow. Thus, in the absence of Particle Image Velocimetry measurements, velocity vector fields can be extracted from image series acquired by the visualization system. Optical flow is an image processing technique for the calculation of velocity fields[6]. With this method, the flow velocity of the observed structures can be estimated using the apparent motion objects in a series of images. The method depends heavily on the changes of grey values in the images such that moving elements are required to maintain a constant brightness from one frame to the next for an accurate calculation of velocities. The method also assumes that the illumination of the images is homogeneous and that the light intensity is constant. Low forcing frequencies enable us to record visualization images in a range between 30 and 250 fps for a relatively long recording time. Depending on the recording rate, one period T which corresponds to 30 or 60 fps, repeats itself 8 or 17 times in a visualization image series consisting of 500 images. Thus, such long image series made it possible to investigate the temporal behavior of basic flow regimes over several cycles.

We employ a gradient-based method for extraction of the optical flow. In this method, the image intensity, I is given by the brightness constraint equation as in Eq. (1).

$$I(x, y, t) = I(x + u\delta t, y + v\delta t, t + \delta t) \tag{1}$$

Expanding the right side of Eq. (1) about the point (x, y, t) in a Taylor series and neglecting the higher-order terms, we obtain a simplified equation for the image intensity as follows,

$$\frac{dI}{dx}u + \frac{dI}{dy}v + \frac{dI}{dt} = 0 \tag{2}$$

Eq. (2) cannot be solved for a single point in the image so some constraints are to be applied. One common constraint is to assume that in a small neighborhood the velocity vector (optical flow) is constant. By combining the pixels in the neighborhood we obtain an over-determined system of equations[7].

$$\begin{bmatrix} \frac{dI}{dx}(1,1) & \frac{dI}{dy}(1,1) \\ \frac{dI}{dx}(1,2) & \frac{dI}{dy}(1,2) \\ . & . \\ . & . \\ \frac{dI}{dx}(N_1, N_2) & \frac{dI}{dy}(N_1, N_2) \end{bmatrix} \begin{bmatrix} u \\ v \end{bmatrix} = \begin{bmatrix} -\frac{dI}{dt}(1,1) \\ -\frac{dI}{dt}(1,2) \\ . \\ . \\ -\frac{dI}{dt}(N_1, N_2) \end{bmatrix} \tag{3}$$

The system in Eq. (3) can be solved using a least-squares based pseudo-inverse method. In Eq. (3), N_1 and N_2 denote the number of pixels in each spatial direction for a selected sub-region. Note that a sub-region containing ($N_1 x N_2$) pixels has the same velocity vector in this sub-region. Too small sub-regions cause insufficient smoothing which leads to noise while too large sub-regions cause too much averaging.

IV. Results

A. Effect of Reynolds number

The actuator plate's frequency *f* determines the value of the Reynolds number, $Re = 2\pi afb/\nu$, if the geometrical parameters are kept constant. This effect is displayed in the visualization images shown in Fig. 3. For low values of Re, the flow is fully periodic and vortical structures are ejected out of the cavity via an oblique jet. With increasing Re, the oblique jet deteriorates and turns into a clockwise rotating vortex flow (See Fig. 3c). Note, that the periodically ejected fluid packets are no longer observable in the vortex flow. For higher values of Re, we observe unsteady flow. We obtained different flow regimes by changing frequency or Reynolds number.

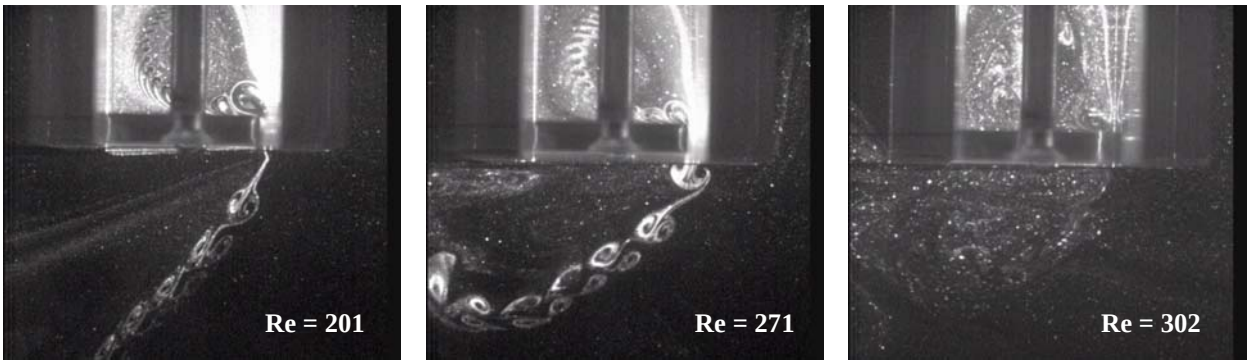

Fig 3. The effect of Reynolds number on the JaVA flow. The actuator plate frequencies are *1 Hz***,** *1.35 Hz* **and** *1.5 Hz* **(from left to right).**

Note that Fig. 3 shows the instantaneous flow field. In order to better understand the flow field for each Re studied, we employ the optical flow approach given in section III to the image (snapshot) series of each experiment in order to obtain instant flow fields. These are then averaged over one cycle in order to get the time-averaged flow field. Figure 4 shows the time-averaged contours of the velocity magnitude and the according vector fields. Fig. 4 clearly shows the transition from an oblique jet to a vortex flow. It is seen that there is a strong clock-wise turning vortex beneath the actuator plate, which may be used to energize a boundary layer in future studies.

To be able to characterize the dynamical behavior of given flows at various frequencies, we performed Fast Fourier Transform (FFT) analyses on a typical point A (shown in Fig. 4). For all three cases in Fig. 3, the total number of existing flow visualization snapshots is 500 and since the recording rate is *30 fps*, it corresponds to a signal length of about 17 cycles. For the use of the FFT technique the number of time samples is required to be a power of 2. This was obtained by using an interpolation method, for which we employed Kriging which is a statistical estimation procedure and uses weighted linear combinations of the available data to estimate unknown values from data observed at known locations[8-9]. Figure 5 shows time histories of the velocity components at point "A" marked in Fig. 4, while figure 6 indicates the according FFT results of these three cases. Note that the coordinate system of the images is defined in such a way that the *y*-axis and the *x*-axis point in *horizontal* and *negative vertical* direction, respectively. As to the results of the FFT, the obtained frequencies are very close to the experimental input data which validates the accuracy of our implementation of the optical flow concept as a robust numerical tool for estimating velocity fields from digital images. The selected point lies on the axis of the oblique jets in all three cases such that the three cases can be compared. Such a comparison indicates that the local flow speeds in the cases with oblique jets are larger than in the vortex regime. For the oblique jet (on the jet) the frequency amplitudes are strong for both components of velocity, while for the vortex mode, on the other hand, the horizontal component of velocity is stronger than the vertical one.

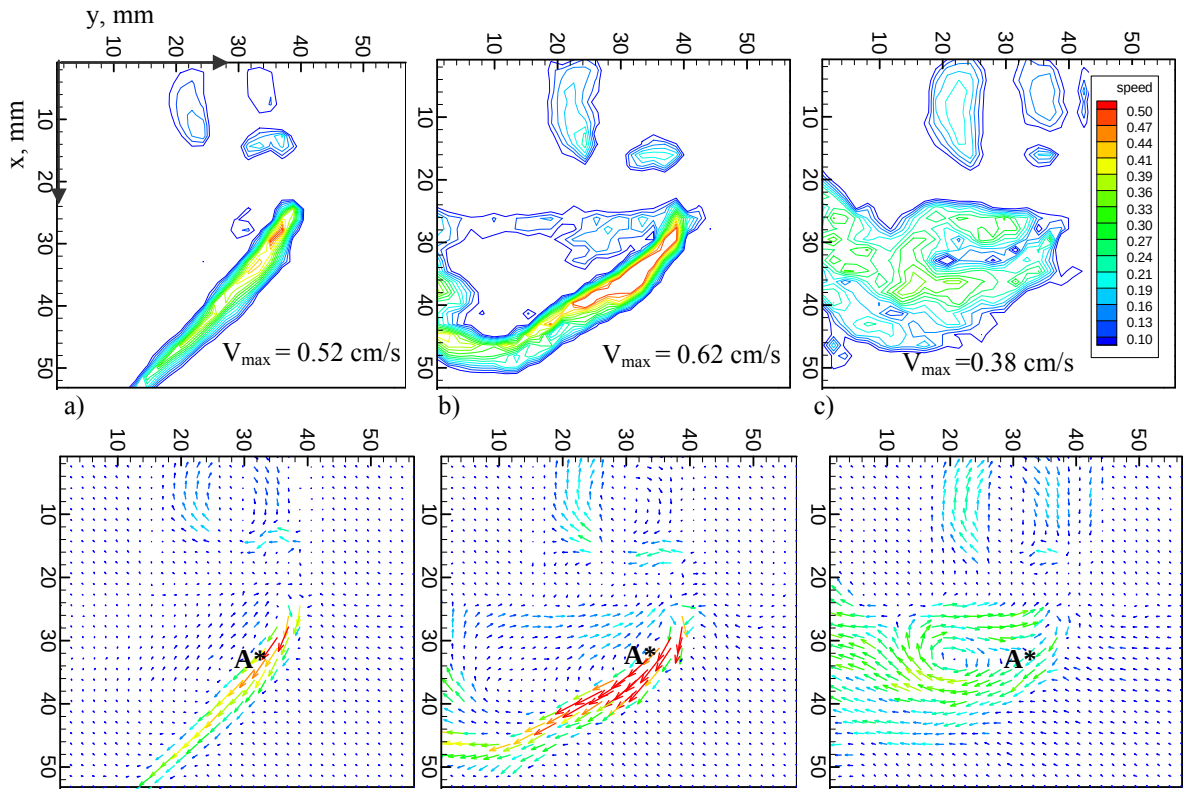

Figure 4. Time-averaged contours of velocity magnitude and vector fields obtained via the optical flow concept. *Velocity magnitude values are given in cm/s a) Re = 201 (1 Hz), b) Re = 271 (1.35 Hz) and c) Re = 302 (1.5 Hz).*

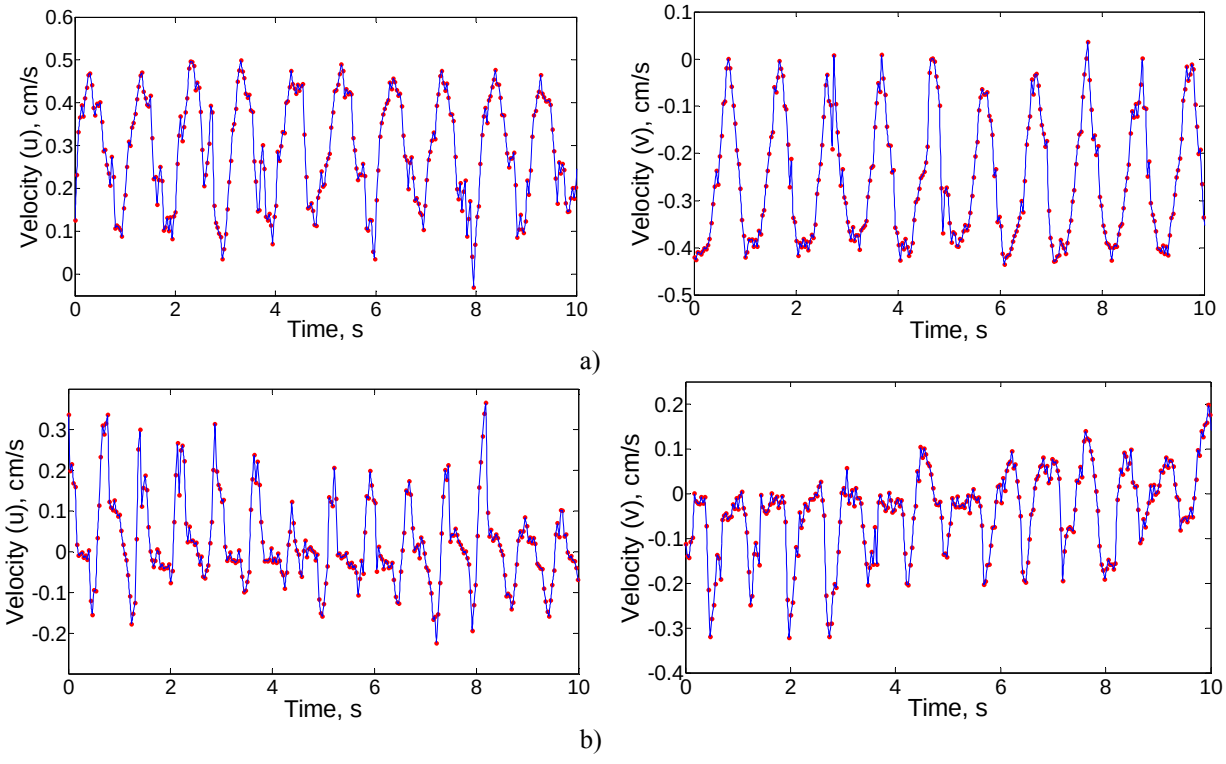

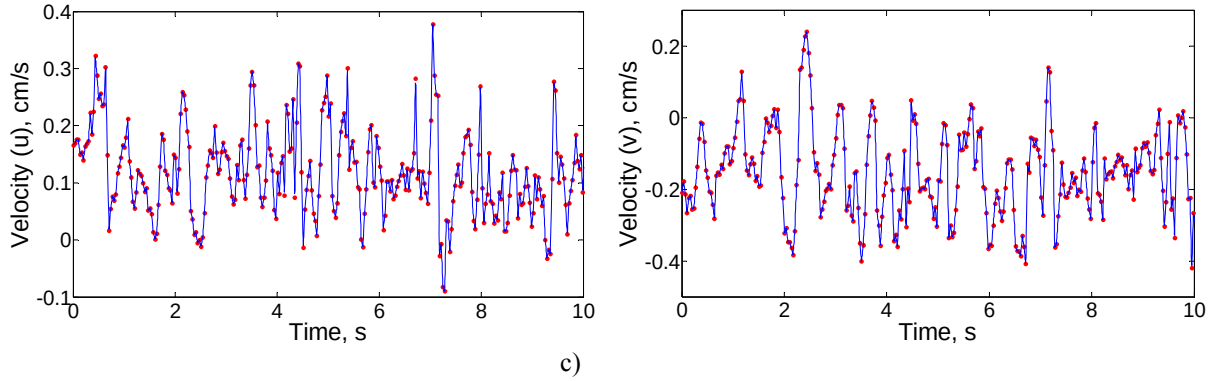

Figure 5. Time histories of velocity components at point A (x = 31.2; y = 33.4) for different values of Re *a) angled jet at 1 Hz, b) transitional (from free jet to vortex mode) jet at 1.35 Hz, c) vortex flow at 1.5 Hz. Left column: Time-histories of vertical velocity component, right column: Time-histories of horizontal velocity component.*

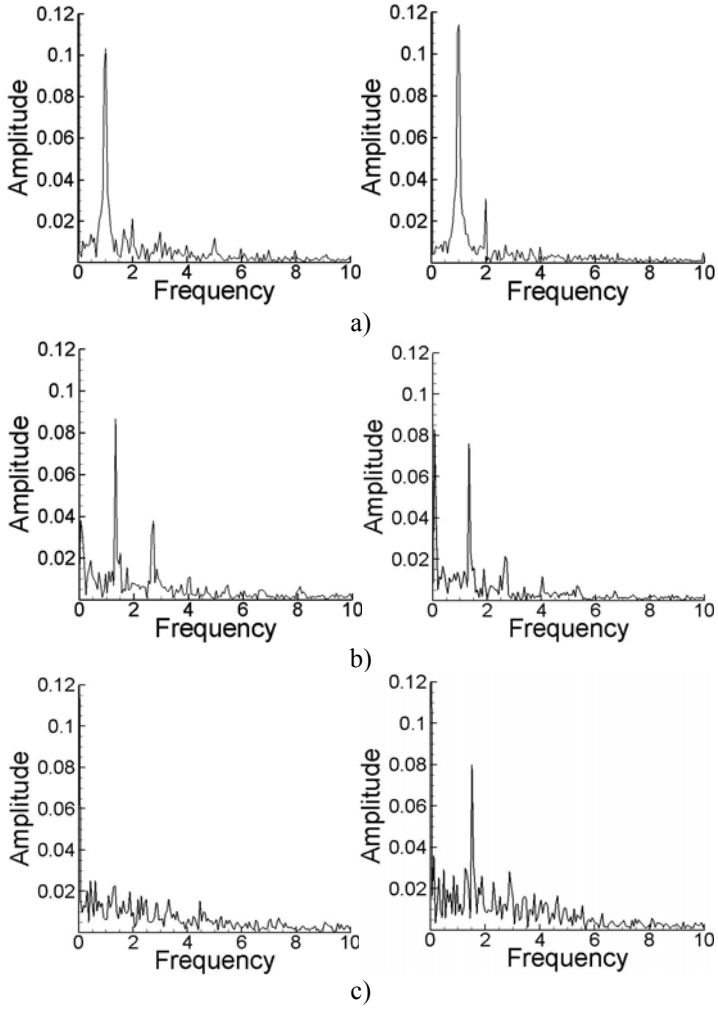

Figure 6. Frequency spectra at point A (x = 31.2; y = 33.4) for different values of Re *a) angled jet at 1 Hz, b) transitional (from free jet to vortex mode) jet at 1.35 Hz, c) vortex flow at 1.5 Hz. Left column: Spectra of vertical velocity component, right column: Spectra of horizontal velocity component.*

B. Effect of Mean Actuator-Plate Position

Our experiments have shown that the JaVA-induced flow regimes are strongly dependent on the mean actuator-plate position as well. In other words, in addition to the governing parameters stated in Ref. 3, the plate's mean position appears to be an additional parameter which deserves to be investigated. For example, one can generate different flow types by changing the mean actuator plate position as shown in Figure 7. Fig. 7a denotes the highest mean position of the plate, Fig. 7b, c and d are each 2 mm lower compared to the previous one. It turns out that as the plate's mean position decreases (i.e., the actuator plate gets retracted deeper into the cavity), the direction of the jet changes from oblique to the right to vertical then to oblique to the left and finally to wall-parallel to the left.

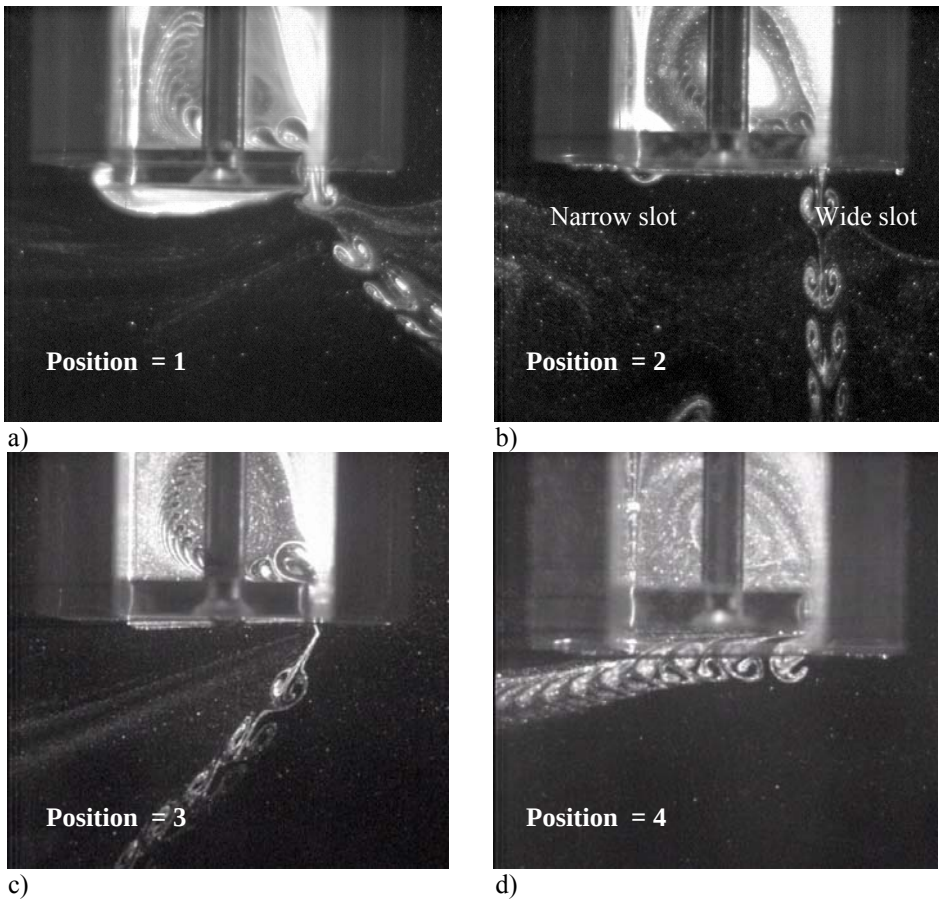

Fig 7. Examples for different actuator flows for an actuation frequency of f = 1 Hz (Re = 201) and different mean actuator-plate positions.

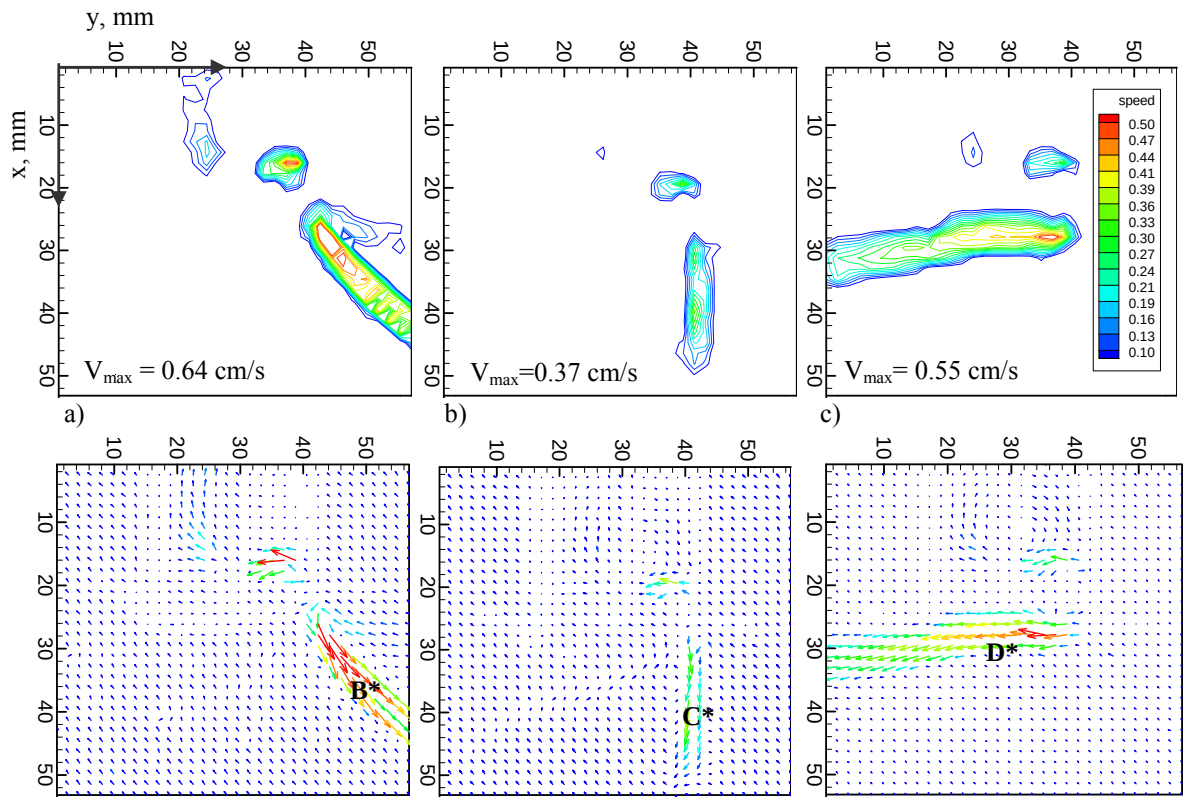

Figure 8. Time-averaged contours of velocity magnitude and vector fields obtained via the optical flow concept. *Velocity magnitude values are given in cm/s a) angled jet to the right (position 1)-60 fps; b) vertical jet (position 2)-30 fps and c) wall jet (position 4)-30 fps.*

Fig. 8 denotes time-averaged contours of velocity magnitude and vector fields for different actuator plate mean positions. It is noted that the strongest jet is the one that is inclined towards the right with a maximum velocity of V_{max} = 0.64 cm/s. The dynamical behavior of the different flow regimes is again investigated by applying the Fourier analysis to points B, C and D selected on the corresponding jet flows in Fig. 8. Figure 9 shows that the velocity components in both directions of the wall jet are periodic, while the vertical jet appears to be noisier than the wall jet, especially for the downward component of velocity (here *u*-component). The FFT analysis gives an idea about the dynamical behavior of the flow regimes if the point to be investigated is appropriately selected to characterize the flow regime.

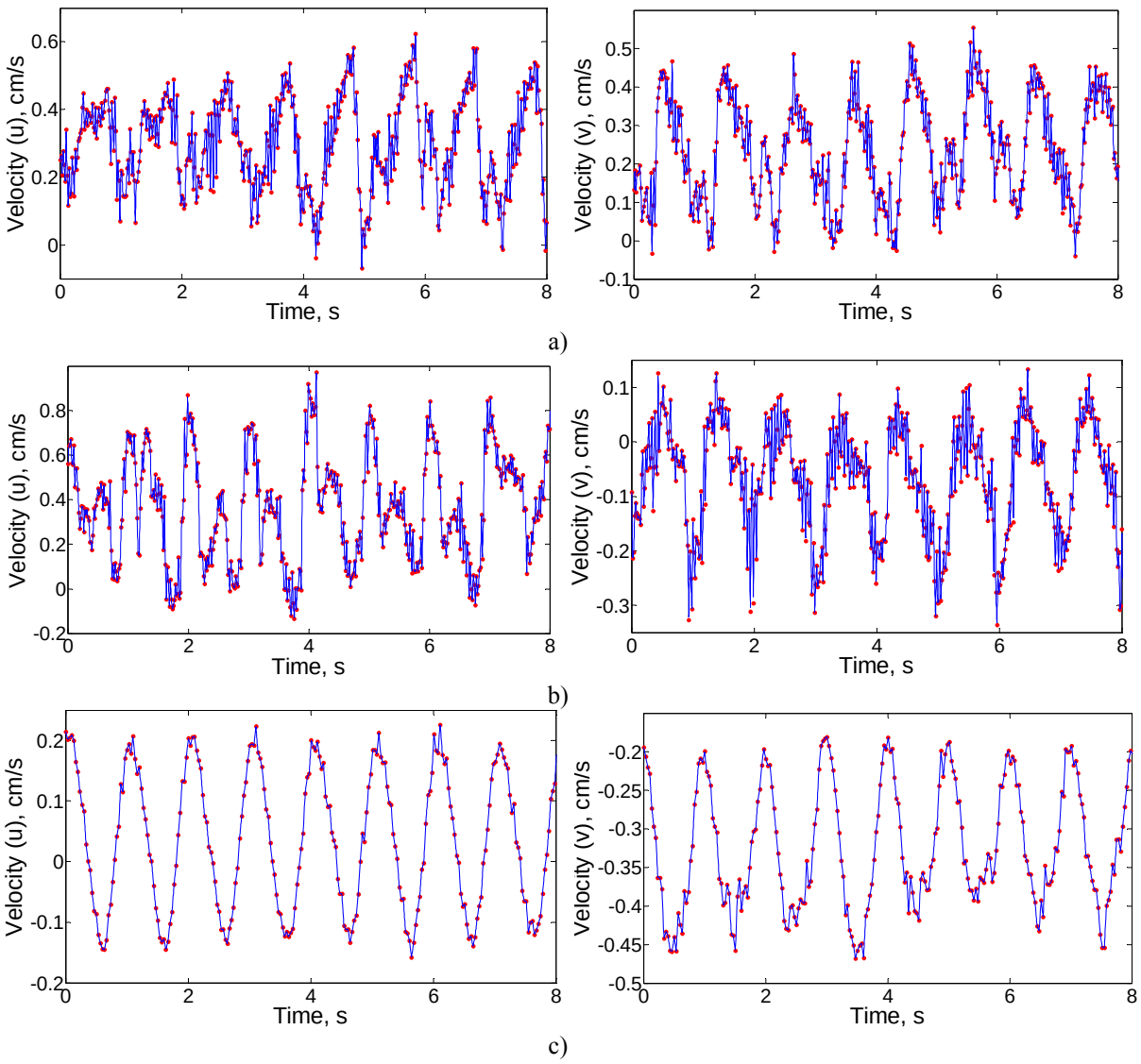

Figure 9. Time histories of velocity components at points B, C and D for different actuator plate mean positions *a) angled jet to the right at B (x = 36.3, y = 49.6), b) vertical jet at C (x = 39.7, y = 40.6), c) wall jet at D (x = 29.5, y = 29.8). Left column: Time-histories of vertical velocity component, right column: Time-histories of horizontal velocity component.*

Fig. 10 shows the according FFT analysis of the data given in Fig. 9. The angled jet to the right has significant peak frequencies in both flow directions. The frequency amplitude is strong for both components and their values are close to each other. The vertical jet on the other hand has a noisy oscillation as shown in Fig. 9 which is characterized by a very strong higher harmonic at *2 Hz* in downward direction of the flow (*u*-component of velocity). We can see in Fig. 9c that the wall jet is periodic and free from noise in both flow directions. Therefore, there are sharp peak frequency amplitudes in both directions with very small harmonics.

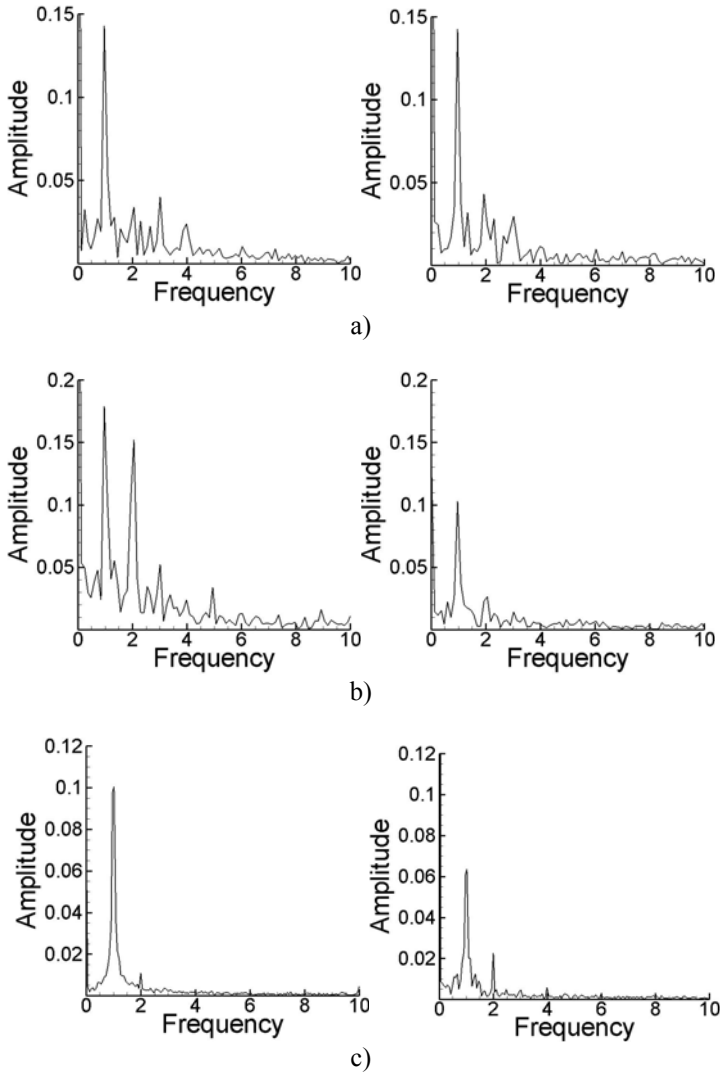

Figure 10. Frequency spectra at points B, C and D for different actuator plate mean positions *a) angled jet to the right at B (x = 36.3, y = 49.6), b) vertical jet at C (x = 39.7, y = 40.6), c) wall jet at D (x = 29.5, y = 29.8). Left column: Spectra of vertical velocity component, right column: Spectra of horizontal velocity component.*

V. Conclusions

As an active flow control device, a Jet and Vortex Actuator (JaVA) has been designed and tested in still water. Unlike Ref. 3, our prototype is designed and manufactured in larger dimensions to operate in water instead of air in order to make it easier to observe flow regimes with naked eye in real time. Depending on geometrical parameters and the actuation frequency, this device produces extremely different flow regimes including oblique, vertical, and wall-parallel jets, as well as vortex flows. This kind of active flow control is supposed to be useful for vortex generation or discrete jet injection for streamwise vortex generation[10]. In this paper we demonstrate that additional parameters that are not mentioned in Ref. 3, e.g. the actuator plate's mean position is an important factor that effects the flow regimes. Therefore, we investigated the effects of this parameter as well as the effects of Reynolds number.

Flow visualizations are done by using fluorescent dye and a high-speed camera. The image series have then been processed quantitatively by the optical flow concept. Fourier analysis and Kriging interpolation are used to study the dynamical behavior of the investigated flow regimes.

Experimental results show that if the frequency of the actuator plate or Reynolds number is increased while keeping other parameters constant, the flow undergoes a transition from an oblique jet to a vortex flow. It is found

that the maximum velocity magnitude occurs for a "transitional" jet flow at $Re = 271$. It is seen that there is a strong clock-wise vortex near the surface of the actuator plate, which may be used to energize a boundary layer.

Changing mean plate position plays a significant role, too. This effect was only discovered recently. All quantitative features mentioned in Ref. 3 have been reproduced but our results are much more detailed and consist of instantaneous velocity fields for quantitative analysis. Thus, the velocity magnitudes show the achievable zones of influence for different flow regimes much clearer and allow a better comparison of different setups, as well as a better basis for their improvement.

Acknowledgements

We are deeply indebted to Francesco Baldani and Bernd Peters for designing, constructing and testing the first version of the JaVA actuator and preparing the experimental set-up and data acquisition system. We also gratefully acknowledge the travel support of Tübitak and the German Ministry of Education and Research (BMBF) that enabled us to perform the present studies, in addition to the support provided by the Universität Stuttgart and Istanbul Technical University.

References

[1]Gad-el-Hak M., "Flow Control – Passive, Active and Reactive Flow Management", Cambridge University Press, 2006.

[2]Taylor, H. D., "Application of Vortex Generator Mixing Principles to Diffusers", Research Department Concluding Report No. R- 15064-5, United Aircraft Corporation, Connecticut, 1948.

[3]Lachowicz J. T., Yao C., Wlezien R. W., "Flow field characterization of a jet and vortex actuator", *Experiments in Fluids*, Vol. 27, 1999, pp. 12 – 20.

[4]Gratzer L. B., "Analysis of Transport Applications for High Lift Schemes" AGARD-LS-43-71, Paper No:7, Rhode Saint Genese, Belgium, 1971

[5]Mc Manus K. and Magill J. "Separation Control in Incompressible and Compressible Flows Using Pulsed Jets", *AIAA Paper* No. 97, Washington D.C., 1971

[6]Horn B. K. P., Schunck B. G. "Determining optical flow", *Artificial Intelligence*, Vol. 17, 1981, pp. 185-203.

[7]Burkhardt, H and Bredebusch, A. "Application of digital image processing methods for the analysis of local structures in fluidized bed processes". Research project C8, 1994.

[8]Gunes, H. and Rist, U. "Spatial resolution enhancement / smoothing of stereo-particle-image-velocimetry data using proper-orthogonal-decomposition-based and Kriging interpolation methods" *Physics of Fluids*, Vol. 19 (6): Art. No. 064101, 2007.

[9]Davis, J.C., "*Statistics and data analysis in Geology*", New York, J. Wiley, 2002.

[10]Wallis R. A., and Stuart C. M., "On the Control of Shock Induced Boundary Layer Separation with Discrete Jets", Aeronautical Research Council Current Paper No. 494, London, Great Britain, 1958.